Physics Letters B ••• (••••) •••–•••

Contents lists available at ScienceDirect

Physics Letters B

www.elsevier.com/locate/physletb

Entropy production and reheating at the chiral phase transition

Christoph Herold [a], Apiwit Kittiratpattana [a], Chinorat Kobdaj [a,*], Ayut Limphirat [a], Yupeng Yan [a], Marlene Nahrgang [b], Jan Steinheimer [c], Marcus Bleicher [c,d,e,f]

[a] School of Physics, Suranaree University of Technology, 111 University Avenue, Nakhon Ratchasima 30000, Thailand
[b] SUBATECH, UMR 6457, Université de Nantes, IMT Atlantique, IN2P3/CNRS, 4 rue Alfred Kastler, 44307 Nantes cedex 3, France
[c] Frankfurt Institute for Advanced Studies, Ruth-Moufang-Str. 1, 60438 Frankfurt am Main, Germany
[d] Institut für Theoretische Physik, Goethe Universität Frankfurt, Max-von-Laue-Strasse 1, D-60438 Frankfurt am Main, Germany
[e] GSI Helmholtzzentrum für Schwerionenforschung GmbH, Planckstr. 1, 64291 Darmstadt, Germany
[f] John von Neumann-Institut für Computing, Forschungzentrum Jülich, 52425 Jülich, Germany

ARTICLE INFO

Article history:
Received 17 August 2018
Received in revised form 4 December 2018
Accepted 4 February 2019
Available online xxxx
Editor: J.-P. Blaizot

Keywords:
Chiral phase transition
Nonequilibrium dynamics
Heavy-ion collisions

ABSTRACT

We study the production of entropy in the context of a nonequilibrium chiral phase transition. The dynamical symmetry breaking is modeled by a Langevin equation for the order parameter coupled to the Bjorken dynamics of a quark plasma. We investigate the impact of dissipation and noise on the entropy and explore the possibility of reheating for crossover and first-order phase transitions, depending on the expansion rate of the fluid. The relative increase in S/N is estimated to range from 10% for a crossover to 200% for a first-order phase transition at low beam energies, which could be detected in the pion-to-proton ratio as a function of beam energy.

1. Introduction

Ultrarelativistic heavy-ion collisions experiments at RHIC and LHC have provided strong evidence for a quark-gluon plasma (QGP) phase at large temperatures and densities. One of the characteristics of this new phase of strongly-interacting matter is the restoration of chiral symmetry which is spontaneously broken in the ground state of quantum chromodynamics (QCD). Lattice QCD studies have revealed a crossover chiral transition for small baryochemical potentials μ_B [1–4], while evidence for a critical point (CP) and first-order phase transition has been obtained from functional methods allowing the exploration of regions with large values of μ_B [5,6]. Up to now, there is no lattice QCD study at physical quark masses that has found a CP or computed the chiral susceptibility at a CP, although some major steps have been undertaken in this direction [7–9]. Recently, considerable progress has been made in constructing a QCD equation of state with a CP based on lattice QCD data [10].

The experimental search for the QCD phase transition is nowadays one of the central goals for current and future collider facilities. It is mainly driven by measurements of net-proton or net-charge multiplicity fluctuations [11–14] which are expected to show characteristic nonmonotonic behavior near the phase transition and especially near the CP where the correlation length diverges [15–23]. A proper understanding of the experimental results, however, requires careful analysis of the dynamical processes that will have an influence especially near a CP where critical slowing down severely limits the growth of the correlation length and therefore of critical fluctuations [24], and memory effects can lead to a broadening of the critical region [25]. Nonequilibrium models have tried to address these issues demonstrating critical slowing down near a CP [26–30] and spinodal decomposition resulting in domain formation at a first-order phase transition [31–35]. Near a CP, the nonequilibrium dynamics will influence the order parameter and, related to that, experimental observables such as net-baryon or net-proton multiplicity fluctuations [23,36,37].

While ideal hydrodynamics preserves the total entropy, the addition of dissipation and fluctuation in nonequilibrium models will lead to an increasing entropy, an effect that is going to be addressed in this paper both qualitatively and quantitatively, together with its potential as an experimental signal for a first-order QCD phase transition. One can expect that a delay in the relaxation of the critical mode produces additional entropy [38]. In this work, we explore the impact of dynamical effects on the production of

* Corresponding author.
E-mail addresses: herold@g.sut.ac.th (C. Herold), kobdaj@g.sut.ac.th (C. Kobdaj).

https://doi.org/10.1016/j.physletb.2019.02.004

entropy within a model describing the realistic dynamics of the chiral transition, the recently studied Nonequilibrium Chiral Fluid Dynamics (NχFD) [39,40]. We investigate the evolution of the critical $k = 0$ mode of the chiral order parameter field coupled to the longitudinal Bjorken-type expansion of a quark–antiquark fluid. The Bjorken model essentially describes a longitudinal fluid dynamical expansion of the fireball created in a heavy-ion collision with the z-component of the fluid velocity given by: $v_z = z/t$ [41]. It should be noted that this approach does not cover various other sources of entropy production such as shear viscosity [42] or compression during the early stage of a heavy-ion collision [43]. Our work is aimed at possible experimental signatures which may confirm or rule out the existence of a CP in systems created in heavy ion collisions. The entropy production in our simulation is mainly a result of the dissipation of the strong fluctuations at the phase transition and CP. This is a generic feature of a non-equilibrium phase transition and should be independent on the exact choice of order parameter. The critical mode in QCD is some mixture of the chiral and baryonic modes and the quark number susceptibilities should diverge at the QCD critical point. This can in principle be described within the dynamics of the chiral quark-meson model for the description of the chiral field dynamics, used in this letter, as shown in [34,35,37,44].

In the present letter we have focussed on the fluctuations of the chiral field, since the sigma field is widely accepted to be the critical mode of the QCD critical point, characterized by a vanishing sigma mass as shown in [22,36]. This work is of Stephanov is one of the fundamental motivations for the beam energy scan program at RHIC [14]. Currently, the volume scaling of the chiral susceptibility is still in agreement with a chiral second-order phase transition in the chiral limit and the divergence of the chiral susceptibility at the CP has also been demonstrated in the QCD inspired NJL model [45].

Results presented in this article are of considerable interest for experiments at the future facilities of FAIR [46], NICA [47], and also for RHIC's BES II program.

The present paper is structured as follows: We present the dynamical equations of our model in Sec. 2 and apply these in Sec. 3 to study the production of entropy from dissipation and fluctuations. Sec. 4 then presents results on the impact of initial conditions on the entropy increase and reheating for crossover and first-order phase transition evolutions. This will be further investigated in Sec. 5 where these effects are compared for different transition scenarios. In the end, we will conclude with a summary and outlook in Sec. 6.

2. Chiral Bjorken dynamics

Our ansatz for the chiral phase transition is the linear sigma or quark-meson model which has the essential features of a crossover for small baryochemical potentials and a CP and first-order phase transition at large values of μ_B. The Lagrangian density of this model is

$$\mathcal{L} = \overline{q}\left(i\gamma^\mu\partial_\mu - g\sigma\right)q + \frac{1}{2}\left(\partial_\mu\sigma\right)^2 - U(\sigma)\,, \tag{1}$$

$$U(\sigma) = \frac{\lambda^2}{4}\left(\sigma^2 - f_\pi^2\right)^2 - f_\pi m_\pi^2\sigma + U_0\,. \tag{2}$$

Here, we have readily set the pion fields equal to their vacuum expectation value of zero as we focus on the evolution of the field σ as the chiral order parameter. The field $q = (u, d)$ includes the light quark fields only. The parameters of this model are chosen in the standard fashion with $f_\pi = 93$ MeV, $m_\pi = 138$ MeV and U_0 such that the potential $U(\sigma)$ vanishes in the ground state. The quark-meson coupling g is fixed by the condition that $g\sigma$ equals the nucleon mass of around 940 MeV in vacuum. We set $\lambda^2 = 19.7$ to fix the mass of the sigma field to 600 MeV.

The equation of motion for the zero mode $\sigma(\tau) = \frac{1}{V}\int \mathrm{d}^3x\sigma(\tau, x)$ reads

$$\ddot{\sigma} + \left(\frac{D}{\tau} + \eta\right)\dot{\sigma} + \frac{\delta\Omega}{\delta\sigma} = \xi\,, \tag{3}$$

with the dot referring to the derivative with respect to proper time τ. The potential $\Omega = U + \Omega_{q\bar{q}}$ contains the mean-field quark–antiquark contribution

$$\Omega_{q\bar{q}} = -2N_f N_c T\int\frac{\mathrm{d}^3p}{(2\pi)^3}\left[\log\left(1 + \mathrm{e}^{-\frac{E-\mu}{T}}\right)\right. \tag{4}$$

$$\left. + \log\left(1 + \mathrm{e}^{-\frac{E+\mu}{T}}\right)\right]\,, \tag{5}$$

with $N_f = 2$, $N_c = 3$ being the number of light quark flavors and colors, T the temperature and $\mu = \mu_B/3$ the quark chemical potential. The dynamically generated energy of a constituent quark with momentum p is $E = \sqrt{p^2 + g^2\sigma^2}$. In the Hubble term $\sim D/\tau$, we set $D = 1$, considering the case of a longitudinal expansion along the direction of the beam axis. The damping coefficient η describes various dissipative processes of the sigma field: First, mesonic interactions, i.e. scattering of a condensed sigma meson with a thermal sigma, $\sigma\sigma \leftrightarrow \sigma\sigma$, and two-pion decay, $\sigma \leftrightarrow \pi\pi$ [48]. Second, meson-quark interactions, $\sigma \leftrightarrow q\bar{q}$ [40]. We include all of these within a phenomenological constant damping coefficient of $\eta = 2.2$/fm [49]. In principle, one could choose a temperature-dependent η as derived in [40]. Its value has been found to be a factor 2–3 larger than our constant value if the system is far away from the phase boundary and approaching zero near the CP which can have significant impact for systems equilibrating in the critical region. For a rapid expansion as we study it here, the impact of a temperature dependence is, however, negligible [27]. The stochastic noise field ξ is assumed to be white and Gaussian, characterized by mean and variance,

$$\langle\xi(t)\rangle = 0\,, \tag{6}$$

$$\langle\xi(t)\xi(t')\rangle = \frac{2T\eta}{V}\delta(t - t')\,. \tag{7}$$

Here, the volume V is given by an expanding cylindrical volume, $V = \pi R^2\tau$, with the radius of a gold nucleus $R = 7.3$ fm to resemble the increasing volume of the fireball created in a central Au + Au collision.

We assume the quark degrees of freedom to constitute an ideal fluid with energy–momentum tensor $T_q^{\mu\nu} = (e + p)u^\mu u^\nu - pg^{\mu\nu}$. Energy–momentum conservation now dictates the vanishing of the divergence of the total energy–momentum tensor,

$$\partial_\mu T^{\mu\nu} = \partial_\mu\left(T_q^{\mu\nu} + T_\sigma^{\mu\nu}\right) = 0\,. \tag{8}$$

A self-consistent derivation within the two-particle irreducible action formalism as in [40] yields

$$\partial_\mu T_q^{\mu\nu} = \left[\frac{\delta\Omega_{q\bar{q}}}{\delta\sigma} + \left(\frac{D}{\tau} + \eta\right)\dot{\sigma}\right]\partial^\nu\sigma\,. \tag{9}$$

Contracting Eq. (9) with the four-velocity u^ν gives the equation for the evolution of the energy density,

$$\dot{e} = -\frac{e + p}{\tau} + \left[\frac{\delta\Omega_{q\bar{q}}}{\delta\sigma} + \left(\frac{D}{\tau} + \eta\right)\dot{\sigma}\right]\dot{\sigma}\,. \tag{10}$$

Please cite this article in press as: C. Herold et al., Entropy production and reheating at the chiral phase transition, Phys. Lett. B (2019), https://doi.org/10.1016/j.physletb.2019.02.004

The net-baryon density follows the equation

$$\dot{n} = -\frac{n}{\tau} \,. \tag{11}$$

Finally, the coupled set of equations (3) and (10) is closed by the equation of state, $p = -\Omega_{q\bar{q}}$. The entropy density at each time τ is then given by

$$s = \frac{e + p - \mu n}{T} \,, \tag{12}$$

and is supposed to yield a conserved total entropy for ideal hydrodynamic evolution. In this case, the equations would need to be modified such that $e = T\frac{\partial p}{\partial T} - p + \mu n + U$ and $p = -\Omega_{q\bar{q}} - U$ together with the condition that the field σ is equal to its equilibrium value at all times. This naturally leads to $s\tau = s_0\tau_0$. The evolution then simply follows the isentropic lines of the quark-meson model as they have been calculated in [50], showing a characteristic bending of trajectories at the phase boundary.

The Langevin equation (3) describes the relaxation of the critical mode. Near equilibrium, neglecting stochastic fluctuations, we may write this as

$$\ddot{\sigma} + \eta\dot{\sigma} + m_\sigma^2(T)\sigma \approx 0 \,. \tag{13}$$

Here, $m_\sigma(T)$ denotes the temperature-dependent screening mass of the sigma meson, defined as the second derivative of Ω with respect to σ at its global minimum. The solution of this equation is given by $\sigma(\tau) \sim \mathrm{e}^{\alpha\tau}$ with

$$\alpha = -\frac{\eta}{2} \pm \sqrt{\frac{\eta^2}{4} - m_\sigma^2(T)} \,. \tag{14}$$

For the underdamped or critically damped case with $m_\sigma(T) \geq \eta/2$, this gives a relaxation time of $2/\eta \approx 0.9$ fm which is prolonged if $m_\sigma(T) < \eta/2$, which is the case around the transition and especially near the CP where $m_\sigma(T) \to 0$ and critical slowing down sets in.

3. Entropy production from dissipation and fluctuations

Besides the full Langevin dynamics, it is instructive to study Eq. (3) without noise ($\xi = 0$) and without dissipation and noise ($\eta = 0$, $\xi = 0$), the latter case representing a propagation according to the classical Euler–Lagrange equation. We choose an initial condition $(T_0, \mu_0) = (171, 19)$ MeV, resulting in an evolution passing through the crossover region of the quark-meson model over a proper time from $\tau = 1$ to 10 fm. The initial entropy-to-baryon number ratio is $S/N = 124.5$ and is constant for ideal hydrodynamics, characterized by the equilibrium condition $\sigma = \sigma_{\mathrm{eq}}$, with

$$\left.\frac{\partial\Omega}{\partial\sigma}\right|_{\sigma=\sigma_{\mathrm{eq}}} = 0 \,. \tag{15}$$

This equation specifies the initial condition for σ. The dynamical treatment of the chiral order parameter, however, raises the expectation that relaxational effects and fluctuations produce entropy during the evolution through and beyond the transition. We show the evolution of $\langle\sigma\rangle$, $\Delta\sigma = \sqrt{\langle(\sigma - \langle\sigma\rangle)^2\rangle}$ and S/N as a function of τ in Fig. 1. Here, $\langle\sigma\rangle$ and $\Delta\sigma$ are scaled by the vacuum expectation value f_π and $\langle\cdot\rangle$ denotes the event-average over different noise configurations which is applied in the case of the full Langevin dynamics. In the upper plot, we can follow the relaxation of the order parameter to equilibrium during the crossover transition. While the scenario without dissipation and noise leads to unphysical fluctuations around equilibrium, the damping term ensures the proper relaxational dynamics. The further addition of a noise term slightly increases the relaxation time, similar to what has been observed in [51] for the Langevin dynamics of the SU(2) deconfining transition. In the behavior of $\Delta\sigma$, we see that the noise also prevents the fluctuations around the equilibrium value to vanish, ensuring that $\Delta\sigma$ remains finite also for later times, when fluctuations in the noise-free case with $\eta > 0$ have already vanished. The initial rapid increase in $\Delta\sigma$ results form the rapid decrease in temperature which the order parameter is not able to follow immediately. The subsequent decay of this fluctuation from $\tau = 2.5$ to 5.5 fm evolves parallel to the rapid increase of σ toward its low-temperature equilibrium value. In the same time, a clear increase in the entropy is seen for the two scenarios with $\eta > 0$, as a result of the energy transfer $\sim \eta\dot{\sigma}$ during the rapid decay of the chirally restored phase. Besides the impact of friction, the plot on the bottom reveals another source of entropy production, namely fluctuations in the order parameter. For the full Langevin dynamics, these seem to produce a steady increase in entropy both before and after the transition process while the large fluctuations around the expectation value in the case without damping and noise leads to a stronger increase due to fluctuations during and after the transition.

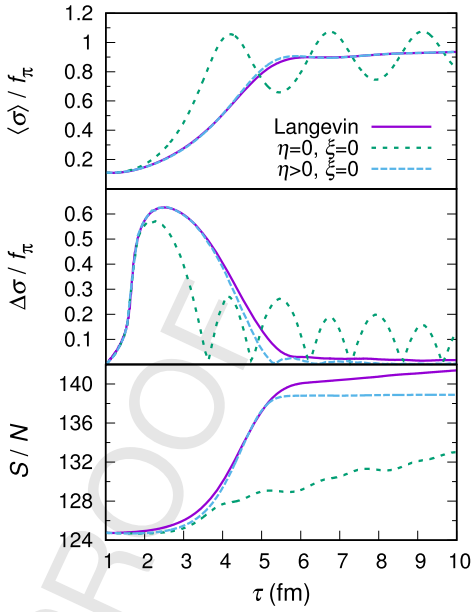

Fig. 1. Top: Event-averaged sigma field. Middle: Fluctuation of the sigma field from equilibrium $\Delta\sigma = \sqrt{\langle(\sigma - \langle\sigma\rangle^2\rangle}$. Bottom: Entropy per baryon as a function of proper time τ, comparing evolutions with a full Langevin dynamics, without dissipation and noise and with dissipation but no noise.

For a 3-dimensional expansion scenario, setting $D = 3$ in Eq. (4) would yield an effectively larger damping and therefore longer relaxation times and a larger amount of entropy produced. This effect would be most significant in the beginning of the expansion, when τ is small. A more realistic description of the volume expansion in a full $(3+1)$-dimensional fluid dynamical simulation is planned and will be presented in a future publication.

4. Impact of the expansion rate

In this section, we are going to investigate the relation between the initial state and the amount of reheating at a crossover and first-order phase transition. We will see that this also has an effect on the evolution of the entropy. We choose three different initial conditions along an isentropic trajectory above the crossover

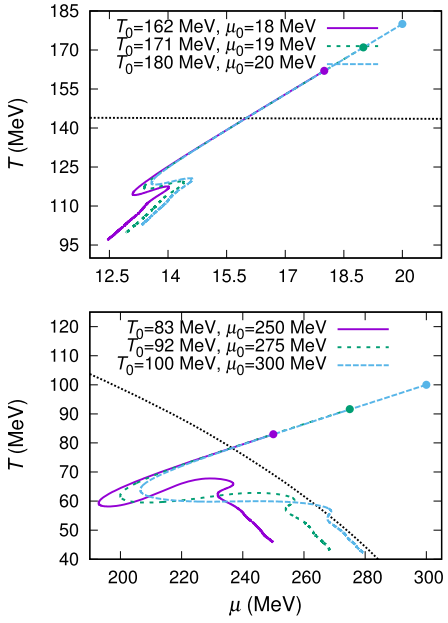

Fig. 2. Top: Event-averaged trajectories for a crossover transition, starting on the same isentropic line but with different distances to the phase boundary. Bottom: Event-averaged trajectories for a first-order phase transition. The dotted line delineates the crossover and first-order phase transition, respectively.

region and the first-order phase transition line, each. The trajectories for these events are shown in two plots in Fig. 2. The first remarkable thing to observe is a reheating process after passing through the crossover, an effect that usually occurs after the decay of a supercooled state in a first-order phase transition. Although no supercooling happens for the dynamical crossover, a delay in the relaxation process during the rapid phase change will nevertheless lead to significant energy dissipation and consequently to an increase in T. We see that the trajectory below the crossover line depends on the initial conditions, trajectories starting closer to the crossover line tend to overshoot the phase boundary further. The reason for this is that for those events, the expansion rate $\sim 1/\tau$ at the phase boundary is larger, i.e. while the relaxation time is roughly the same, the more rapid expansion leads to a lower T and μ before the relaxation process to the chirally broken phase starts. At a first-order phase transition, the overshooting effect is the same and has also been found before in inhomogeneous media [35]. In contrast to the crossover, however, we can see a clearer difference in the evolution below the phase transition line. Starting closer to the phase boundary leads to a stronger reheating process which can here be ascribed to the formation and decay of a supercooled state. The longer this state survives, the larger amount of energy will be dissipated into the fluid causing a larger rise in the temperature. In the context of heavy-ion experiments, it is important to understand this effect as it will create additional thermal background. Finally, we note that significantly higher values of μ are reached by choosing an initial state farther away from the first-order phase transition line.

Fig. 3 shows the evolution of S/S_0. Here, we consider the relative increase in entropy by dividing through the initial entropy of the medium $S_0 \equiv S$ ($\tau = 1$ fm). We see that, in general, the entropy increases stronger at a first-order phase transition than at a crossover. Furthermore, the amount of increase depends on how close the initial condition is to the phase boundary, with a higher expansion rate resulting in a larger increase in S.

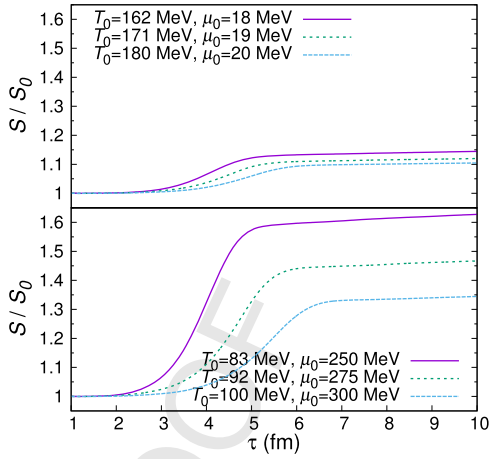

Fig. 3. Top: Event-averaged entropy increase for a crossover scenario, corresponding to the trajectories in Fig. 2 (top). Bottom: Event-averaged entropy increase for a first-order phase transition, corresponding to the trajectories in Fig. 2 (bottom).

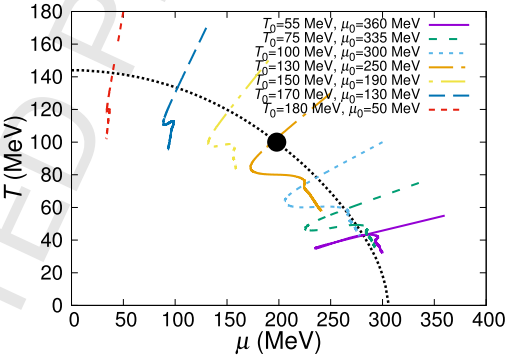

Fig. 4. Event-averaged trajectories for several initial conditions, probing different regions of the phase diagram. The dashed line corresponds to the phase boundary and the black dot indicates the position of the CP.

5. Entropy increase with and without latent heat

We are now prepared to estimate the entropy production for events with different initial densities, probing different regions of the phase diagram. To make the results comparable, we are choosing initial conditions all across the phase diagram in such a way that each trajectory is going to meet the phase boundary at a fixed proper time of $\tau = 2$ fm. Although this does not necessarily reflect the experimental reality where the initial condition is solely determined by the beam energy and nucleon number, this will help us disentangle effects of different transition types from the impact of the expansion rate discussed in the previous section. The trajectories are shown in Fig. 4, together with the corresponding evolution of S/S_0 in Fig. 5. A clear trend is found: While for a crossover and CP transition the entropy increase is of the order of 10–20%, slowly becoming larger for transitions closer to the CP, the presence of a latent heat amplifies this effect, resulting in an increase of up to 100% for the trajectory with the strongest first-order phase transition.

Experimentally, this effect can be expected to lead to an increase of the pion-to-baryon-number ratio, we therefore propose future experiments to search for steps in the π/p multiplicity ratio as function of the beam energy.

Please cite this article in press as: C. Herold et al., Entropy production and reheating at the chiral phase transition, Phys. Lett. B (2019), https://doi.org/10.1016/j.physletb.2019.02.004

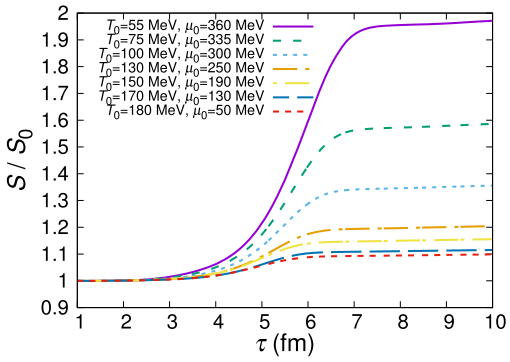

Fig. 5. Relative entropy increase for the trajectories shown in Fig. 4. We see that with increasing initial μ, the entropy increase becomes more significant.

6. Conclusions

We have studied the dynamical evolution of the zero mode of the chiral order parameter σ during the longitudinal expansion of a hot and dense fluid, described by the coupling to Bjorken hydrodynamics. The results demonstrate that entropy is generated by damping processes during the transition and by stochastic fluctuations during the whole evolution. Interestingly, a reheating effect of the medium is observed not only for a first-order phase transition but also for events with a crossover. In all cases, the amount of reheating and entropy production depends on the expansion rate at the moment when the medium reaches the phase boundary. Assuming a proper time interval of ~ 1 fm between the thermalization of the medium and the start of the transition process, we were able to estimate the relative increase of S/N ranging from 25% for a crossover to up to 200% for a first-order phase transition.

As the present study is a very simple model for the production of entropy, more realistic approaches should be pursued in the future. Possible extensions of this work should consider an inhomogeneous medium, i.e. a full $(3+1)$-dimensional hydrodynamic expansion and include the effect of spatial fluctuations or higher-order modes of the chiral order parameter field.

Acknowledgements

This work was supported by Suranaree University of Technology (SUT), TRF-RGJ, Deutscher Akademischer Austauschdienst (DAAD), HIC for FAIR and in the framework of COST Action CA15213 THOR. C.H. and C.K. acknowledge support from SUT-CHE-NRU (FtR.15/2559) project. M.N. acknowledges the support of the program “Etoiles montantes en Pays de la Loire 2017”.

References

[1] Y. Aoki, G. Endrodi, Z. Fodor, S.D. Katz, K.K. Szabo, The order of the quantum chromodynamics transition predicted by the standard model of particle physics, Nature 443 (2006) 675–678, https://doi.org/10.1038/nature05120, arXiv:hep-lat/0611014.
[2] S. Borsanyi, et al., Is there still any T_c mystery in lattice QCD? Results with physical masses in the continuum limit III, J. High Energy Phys. 1009 (2010) 073, https://doi.org/10.1007/JHEP09(2010)073, arXiv:1005.3508.
[3] S. Borsanyi, Z. Fodor, C. Hoelbling, S.D. Katz, S. Krieg, K.K. Szabo, Full result for the QCD equation of state with $2+1$ flavors, Phys. Lett. B 730 (2014) 99–104, https://doi.org/10.1016/j.physletb.2014.01.007, arXiv:1309.5258.
[4] A. Bazavov, et al., Equation of state in $(2+1)$-flavor QCD, Phys. Rev. D 90 (9) (2014) 094503, https://doi.org/10.1103/PhysRevD.90.094503, arXiv:1407.6387.
[5] C.S. Fischer, J. Luecker, Propagators and phase structure of Nf = 2 and Nf = 2 + 1 QCD, Phys. Lett. B 718 (2013) 1036–1043, https://doi.org/10.1016/j.physletb.2012.11.054, arXiv:1206.5191.
[6] F. Gao, Y.-x. Liu, QCD phase transitions via a refined truncation of Dyson–Schwinger equations, Phys. Rev. D 94 (7) (2016) 076009, https://doi.org/10.1103/PhysRevD.94.076009, arXiv:1607.01675.
[7] Y. Aoki, S. Borsanyi, S. Durr, Z. Fodor, S.D. Katz, et al., The QCD transition temperature: results with physical masses in the continuum limit II, J. High Energy Phys. 0906 (2009) 088, https://doi.org/10.1088/1126-6708/2009/06/088, arXiv:0903.4155.
[8] S. Datta, R.V. Gavai, S. Gupta, The QCD critical point: marching towards continuum, Nucl. Phys. A 904–905 (2013) 883c–886c, https://doi.org/10.1016/j.nuclphysa.2013.02.156, arXiv:1210.6784.
[9] A. Bazavov, H.T. Ding, P. Hegde, F. Karsch, E. Laermann, S. Mukherjee, P. Petreczky, C. Schmidt, Chiral phase structure of three flavor QCD at vanishing baryon number density, Phys. Rev. D 95 (7) (2017) 074505, https://doi.org/10.1103/PhysRevD.95.074505, arXiv:1701.03548.
[10] P. Parotto, M. Bluhm, D. Mroczek, M. Nahrgang, J. Noronha-Hostler, K. Rajagopal, C. Ratti, T. Schäfer, M. Stephanov, Lattice-QCD-based equation of state with a critical point, arXiv:1805.05249.
[11] M. Aggarwal, et al., Higher moments of net-proton multiplicity distributions at RHIC, Phys. Rev. Lett. 105 (2010) 022302, https://doi.org/10.1103/PhysRevLett.105.022302, arXiv:1004.4959.
[12] X. Luo, Search for the QCD critical point by higher moments of net-proton multiplicity distributions at STAR, arXiv:1210.5573.
[13] L. Adamczyk, et al., Energy dependence of moments of net-proton multiplicity distributions at RHIC, Phys. Rev. Lett. 112 (2014) 032302, https://doi.org/10.1103/PhysRevLett.112.032302, arXiv:1309.5681.
[14] X. Luo, Energy dependence of moments of net-proton and net-charge multiplicity distributions at STAR, PoS CPOD2014 (2014) 019, arXiv:1503.02558.
[15] M. Asakawa, U.W. Heinz, B. Muller, Fluctuation probes of quark deconfinement, Phys. Rev. Lett. 85 (2000) 2072–2075, https://doi.org/10.1103/PhysRevLett.85.2072, arXiv:hep-ph/0003169.
[16] M.A. Stephanov, K. Rajagopal, E.V. Shuryak, Signatures of the tricritical point in QCD, Phys. Rev. Lett. 81 (1998) 4816–4819, https://doi.org/10.1103/PhysRevLett.81.4816, arXiv:hep-ph/9806219.
[17] M.A. Stephanov, K. Rajagopal, E.V. Shuryak, Event-by-event fluctuations in heavy ion collisions and the QCD critical point, Phys. Rev. D 60 (1999) 114028, https://doi.org/10.1103/PhysRevD.60.114028, arXiv:hep-ph/9903292.
[18] M. Cheng, et al., Baryon number, strangeness and electric charge fluctuations in QCD at high temperature, Phys. Rev. D 79 (2009) 074505, https://doi.org/10.1103/PhysRevD.79.074505, arXiv:0811.1006.
[19] M. Asakawa, S. Ejiri, M. Kitazawa, Third moments of conserved charges as probes of QCD phase structure, Phys. Rev. Lett. 103 (2009) 262301, https://doi.org/10.1103/PhysRevLett.103.262301, arXiv:0904.2089.
[20] S. Gupta, X. Luo, B. Mohanty, H.G. Ritter, N. Xu, Scale for the phase diagram of quantum chromodynamics, Science 332 (2011) 1525–1528, https://doi.org/10.1126/science.1204621, arXiv:1105.3934.
[21] B. Friman, F. Karsch, K. Redlich, V. Skokov, Fluctuations as probe of the QCD phase transition and freeze-out in heavy ion collisions at LHC and RHIC, Eur. Phys. J. C 71 (2011) 1694, https://doi.org/10.1140/epjc/s10052-011-1694-2, arXiv:1103.3511.
[22] M.A. Stephanov, Non-Gaussian fluctuations near the QCD critical point, Phys. Rev. Lett. 102 (2009) 032301, https://doi.org/10.1103/PhysRevLett.102.032301, arXiv:0809.3450.
[23] C. Athanasiou, K. Rajagopal, M. Stephanov, Using higher moments of fluctuations and their ratios in the search for the QCD critical point, Phys. Rev. D 82 (2010) 074008, https://doi.org/10.1103/PhysRevD.82.074008, arXiv:1006.4636.
[24] B. Berdnikov, K. Rajagopal, Slowing out-of-equilibrium near the QCD critical point, Phys. Rev. D 61 (2000) 105017, https://doi.org/10.1103/PhysRevD.61.105017, arXiv:hep-ph/9912274.
[25] C. Herold, M. Bleicher, M. Nahrgang, J. Steinheimer, A. Limphirat, C. Kobdaj, Y. Yan, Broadening of the chiral critical region in a hydrodynamically expanding medium, Eur. Phys. J. A 54 (2) (2018) 19, https://doi.org/10.1140/epja/i2018-12438-1, arXiv:1710.03118.
[26] M. Nahrgang, S. Leupold, M. Bleicher, Equilibration and relaxation times at the chiral phase transition including reheating, Phys. Lett. B 711 (2012) 109–116, https://doi.org/10.1016/j.physletb.2012.03.059, arXiv:1105.1396.
[27] C. Herold, M. Nahrgang, I.N. Mishustin, M. Bleicher, Chiral fluid dynamics with explicit propagation of the Polyakov loop, Phys. Rev. C 87 (2013) 014907, https://doi.org/10.1103/PhysRevC.87.014907, arXiv:1301.1214.
[28] S. Mukherjee, R. Venugopalan, Y. Yin, Real time evolution of non-Gaussian cumulants in the QCD critical regime, Phys. Rev. C 92 (3) (2015) 034912, https://doi.org/10.1103/PhysRevC.92.034912, arXiv:1506.00645.
[29] M. Stephanov, Y. Yin, Hydrodynamics and critical slowing down, Nucl. Phys. A 967 (2017) 876–879, https://doi.org/10.1016/j.nuclphysa.2017.06.051, arXiv:1704.07396.
[30] M. Nahrgang, M. Bluhm, T. Schäfer, S.A. Bass, Diffusive dynamics of critical fluctuations near the QCD critical point, arXiv:1804.05728.
[31] J. Randrup, Phase transition dynamics for baryon-dense matter, Phys. Rev. C 79 (2009) 054911, https://doi.org/10.1103/PhysRevC.79.054911, arXiv:0903.4736.

[32] J. Randrup, Spinodal phase separation in relativistic nuclear collisions, Phys. Rev. C 82 (2010) 034902, https://doi.org/10.1103/PhysRevC.82.034902, arXiv:1007.1448.
[33] J. Steinheimer, J. Randrup, Spinodal amplification of density fluctuations in fluid-dynamical simulations of relativistic nuclear collisions, Phys. Rev. Lett. 109 (2012) 212301, https://doi.org/10.1103/PhysRevLett.109.212301, arXiv:1209.2462.
[34] C. Herold, M. Nahrgang, I. Mishustin, M. Bleicher, Formation of droplets with high baryon density at the QCD phase transition in expanding matter, Nucl. Phys. A 925 (2014) 14–24, https://doi.org/10.1016/j.nuclphysa.2014.01.010, arXiv:1304.5372.
[35] C. Herold, M. Nahrgang, Y. Yan, C. Kobdaj, Net-baryon number variance and kurtosis within nonequilibrium chiral fluid dynamics, J. Phys. G 41 (11) (2014) 115106, https://doi.org/10.1088/0954-3899/41/11/115106, arXiv:1407.8277.
[36] M. Stephanov, On the sign of kurtosis near the QCD critical point, Phys. Rev. Lett. 107 (2011) 052301, https://doi.org/10.1103/PhysRevLett.107.052301, arXiv:1104.1627.
[37] C. Herold, M. Nahrgang, Y. Yan, C. Kobdaj, Dynamical net-proton fluctuations near a QCD critical point, Phys. Rev. C 93 (2) (2016) 021902, https://doi.org/10.1103/PhysRevC.93.021902, arXiv:1601.04839.
[38] L.P. Csernai, J.I. Kapusta, Dynamics of the QCD phase transition, Phys. Rev. Lett. 69 (1992) 737–740, https://doi.org/10.1103/PhysRevLett.69.737.
[39] I.N. Mishustin, O. Scavenius, Chiral fluid dynamics and collapse of vacuum bubbles, Phys. Rev. Lett. 83 (1999) 3134–3137, https://doi.org/10.1103/PhysRevLett.83.3134, arXiv:hep-ph/9804338.
[40] M. Nahrgang, S. Leupold, C. Herold, M. Bleicher, Nonequilibrium chiral fluid dynamics including dissipation and noise, Phys. Rev. C 84 (2011) 024912, https://doi.org/10.1103/PhysRevC.84.024912, arXiv:1105.0622.
[41] J.D. Bjorken, Highly relativistic nucleus–nucleus collisions: the central rapidity region, Phys. Rev. D 27 (1983) 140–151, https://doi.org/10.1103/PhysRevD.27.140, https://link.aps.org/doi/10.1103/PhysRevD.27.140.
[42] A. Dumitru, E. Molnar, Y. Nara, Entropy production in high-energy heavy-ion collisions and the correlation of shear viscosity and thermalization time, Phys. Rev. C 76 (2007) 024910, https://doi.org/10.1103/PhysRevC.76.024910, arXiv:0706.2203.
[43] M. Reiter, A. Dumitru, J. Brachmann, J.A. Maruhn, H. Stoecker, W. Greiner, Entropy production in collisions of relativistic heavy ions: a signal for quark gluon plasma phase transition?, Nucl. Phys. A 643 (1998) 99–112, https://doi.org/10.1016/S0375-9474(98)00556-9, arXiv:nucl-th/9806010.
[44] C. Herold, M. Nahrgang, C. Kobdaj, A. Limphirat, Y. Yan, Evolution of critical fluctuations in a heavy-ion collision scenario, Nucl. Phys. A 967 (2017) 828–831, https://doi.org/10.1016/j.nuclphysa.2017.05.065.
[45] K. Fukushima, Chiral effective model with the Polyakov loop, Phys. Lett. B 591 (2004) 277–284, https://doi.org/10.1016/j.physletb.2004.04.027, arXiv:hep-ph/0310121.
[46] B. Friman, C. Hohne, J. Knoll, S. Leupold, J. Randrup, et al., The CBM physics book: compressed baryonic matter in laboratory experiments, Lect. Notes Phys. 814 (2011) 1–980, https://doi.org/10.1007/978-3-642-13293-3.
[47] theor.jinr.ru/twiki-cgi/view/NICA/NICAWhitePaper.
[48] L.P. Csernai, P.J. Ellis, S. Jeon, J.I. Kapusta, Dynamical evolution of the scalar condensate in heavy ion collisions, Phys. Rev. C 61 (2000) 054901, https://doi.org/10.1103/PhysRevC.61.054901, arXiv:nucl-th/9908020.
[49] T.S. Biro, C. Greiner, Dissipation and fluctuation at the chiral phase transition, Phys. Rev. Lett. 79 (1997) 3138–3141, https://doi.org/10.1103/PhysRevLett.79.3138, arXiv:hep-ph/9704250.
[50] O. Scavenius, A. Mocsy, I.N. Mishustin, D.H. Rischke, Chiral phase transition within effective models with constituent quarks, Phys. Rev. C 64 (2001) 045202, https://doi.org/10.1103/PhysRevC.64.045202, arXiv:nucl-th/0007030.
[51] E.S. Fraga, G. Krein, A.J. Mizher, Langevin dynamics of the pure SU(2) deconfining transition, Phys. Rev. D 76 (2007) 034501, https://doi.org/10.1103/PhysRevD.76.034501, arXiv:0705.0226.

Please cite this article in press as: C. Herold et al., Entropy production and reheating at the chiral phase transition, Phys. Lett. B (2019), https://doi.org/10.1016/j.physletb.2019.02.004